Wind and Structures, *Vol. 20, No. 5 (2015) 609-622*
DOI: http://dx.doi.org/10.12989/was.2015.20.5.609

Improved modeling of equivalent static loads on wind turbine towers

Kuangmin Gong and Xinzhong Chen*

National Wind Institute, Department of Civil and Environmental Engineering, Texas Tech University, Lubbock, TX 79409, USA

(Received October 10, 2014, Revised February 6, 2015, Accepted February 7, 2015)

Abstract. This study presents a dynamic response analysis of operational and parked wind turbines in order to gain better understanding of the roles of wind loads on turbine blades and tower in the generation of turbine response. The results show that the wind load on the tower has a negligible effect on the blade responses of both operational and parked turbines. Its effect on the tower response is also negligible for operational turbine, but is significant for parked turbine. The tower extreme responses due to the wind loads on blades and tower of parked turbine can be estimated separately and then combined for the estimation of total tower extreme response. In current wind turbine design practice, the tower extreme response due to the wind loads on blades is often represented as a static response under an equivalent static load in terms of a concentrated force and a moment at the tower top. This study presents an improved equivalent static load model with additional distributed inertial force on tower, and introduces the square-root-of-sum-square combination rule, which is shown to provide a better prediction of tower extreme response.

Keywords: extreme response; wind loading; equivalent static loads; combination rule; wind turbine

1. Introduction

With increases in size and flexibility of utility-scale wind turbines, especially for offshore applications, a better understanding of dynamic interaction between turbine components is increasingly important for the assessment of turbine performance to ensure structural safety and serviceability. In current turbine design practice, aeroelastic analysis tools such FAST (Fatigue, Aerodynamics, Structures, and Turbulence) code (Jonkman and Buhl 2005, Moriarty 2008) are often used to quantify turbine dynamic response for given wind inflows, in which a nonlinear aerodynamic force model is used to define the aerodynamic forces on blades (Moriarty and Hansen 2005), and the structural dynamic coupling of wind turbine tower and blades is adequately modeled. The wind load on tower is often neglected when assessing blade response. In current practice, the tower extreme response due to aerodynamic loads on blades is often represented as a static response under equivalent static loads (ESLs) in terms of a concentrated force and a moment at the tower top. The tower responses caused by the concentrated force and moment are assumed to be fully correlated thus can be added together (DNV and Risø 2002). It is then combined with

*Corresponding author, Professor, E-mail: xinzhong.chen@ttu.edu

http://www.techno-press.org/?journal=was&subpage=8 ISSN: 1226-6116 (Print), 1598-6225 (Online)

the tower response due to the wind load on tower only for the estimation of total tower response. This equivalent static load approach also facilitates combinations with other responses (loads) important for the tower design (Holmes 2002, Chen and Kareem 2004, Huang and Chen 2007, Katsumura *et al*. 2007, Li *et al*. 2009, Zhou *et al*. 2011, Blaise and Denoel 2013). The along-wind response of an operational wind turbine tower with blade coupling was also addressed in Murtagh *et al*. (2005), where a simplified quasi-steady drag force model was used to define the aerodynamic forces on the rotating blades. The time histories of the drag forces were directly calculated from the time histories of along-wind turbulence, which were generated using the rotationally sampled spectra. As illustrated in Murtagh *et al*. (2005) among others, exclusion of blade/tower interaction can considerably underestimate the response at the tower top, especially, when the frequencies of blades and tower are close to each other.

This study addresses the roles of wind loads on blades and tower in the generation of dynamic responses of turbine system under both operational and parked conditions. The wind turbine used in this analysis is the National Renewable Energy Laboratory (NREL) onshore 5-MW baseline wind turbine (Jonkman *et al*. 2009), which is modeled as a multi-degree-of-freedom (MDOF) system in FAST code (recompiled to consider wind load on tower). The stationary Gaussian wind turbulence fields were generated based on spectral representation method (Shinozuka and Deodatis 1996, Chen and Kareem 2005). Three different dynamic response analyses were carried out in terms of different consideration of the wind loads: Case 1: Wind loads on both the tower and blades; Case 2: Wind loads on the blades only; and Case 3: Wind load on the tower only. The turbine responses of those three cases are compared. The mean extreme response of the tower was estimated by the combination of extreme responses derived from Cases 2 and 3, and compared with that from Case 1. The adequacy of current assumption of full correlation between tower responses caused by the concentrated force and moment at the tower top (DNV and Risø 2002) is examined. Furthermore, an improved ESL modeling in terms of concentrated force and moment and distributed modal inertial load is established for a better prediction of the tower extreme response caused by the wind loads on blades. The results of this study also help in better understanding the unique dynamic response characteristics of wind turbines which are different from those of other wind-excited structures such as tall buildings.

2. Characteristics of wind turbine and wind inflow

The NREL onshore 5-MW baseline wind turbine is an upwind 3-blade wind turbine with a rotor diameter of 126 m, a hub height of 90 m and tower height of 87.6 m. It uses variable-speed and collective pitch-control configuration with rated wind speed of 11.4 m/s and rated rotor speed of 12.1 rpm. The turbine operating wind speed range is between cut-in of 3 m/s and cut-out of 25 m/s. The yaw angle is set to zero degree during normal operational and parked conditions. The pitch angle at normal parked condition is 90 degrees. The wind turbine was modeled by a combined modal and multi-body dynamics formulation, with 16 degrees of freedom (DOFs), including three DOFs of each blade: 1^{st} and 2^{nd} flapwise modes, and 1^{st} edgewise mode; four DOFs of tower: 1^{st} and 2^{nd} tower fore-aft (FA) modes, 1^{st} and 2^{nd} tower side-to-side (SS) modes; one DOF of nacelle yaw motion; one DOF of generator azimuth angle; one DOF of drive train rotational-flexibility. The tower is assumed to be rigidly fixed to the ground. The blade flap-wise and edge-wise directions are referred to the directions normal to and along with the chord line of airfoil as shown in Fig. 1. For the operational turbine, the pitch angle varies with wind speed from

zero to 23.47 degrees due to a pitch control scheme. With zero pitch angle, the flap-wise and edge-wise directions correspond to out of and in the rotor plane, respectively. Therefore, the flap-wise root bending moment and tower FA bending moment are also referred to as out-of-plane responses, while the edge-wise root bending moment and tower SS bending moment are in-plane responses. On the contrary, for a parked turbine with a pitch angle of 90 degrees, the flap-wise and edge-wise directions correspond to in and out of the rotor plane, respectively.

A random wind turbulence field with *u*-, *v*- and *w*-components was simulated at a 31-by-31 grid points, with both height and width of 145 m and a single column grid points along the tower as shown in Fig. 2. The hub is located at the center of grid. The grid area is sufficient to cover the rotor when considering the possibility of yaw and tilt. The wind conditions for operational and parked turbines are chosen according to the IEC standard (IEC 61400-1:2005) as wind turbine design load condition (DLC) 1.1 with normal turbulence model (NTM), and DLC 6.1 with extreme wind speed model (EWM), respectively. The Kaimal spectrum of turbulence is used for wind turbine class I with a category A. The *u*-, *v*- and *w*-components of turbulence are assumed to be independent. The coherence function for *u*-component is described by the exponential coherence model, while those of *v*- and *w*-components are not considered (Jonkman 2009). The standard derivation (STD) of *u*-component is $\sigma_u = 0.16(0.75U_{\text{hub}} + 5.6)$ for operational turbine, and $\sigma_u = 0.11U_{\text{hub}}$ for parked turbine, where U_{hub} is the mean wind speed at hub height. The STDs of *v*- and *w*-components are $\sigma_v = 0.8\sigma_u$ and $\sigma_w = 0.5\sigma_u$. The STDs of wind turbulence components are assumed to be invariant in whole wind field. The integral length scales of *u*-, *v*- and *w*-components of turbulence are 340.2 m, 113.4 m and 27.7 m. The mean wind speed profile is given by a power law with exponents of 0.2 and 0.11 for operational and parked turbines, respectively.

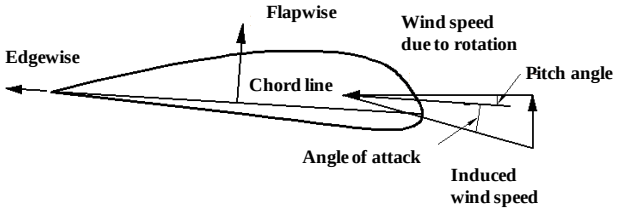

Fig. 1 Terminology of airfoil

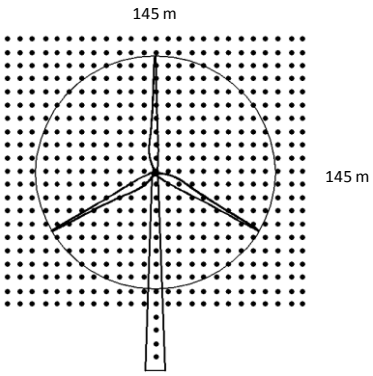

Fig. 2 Grid points for simulating random wind turbulence field

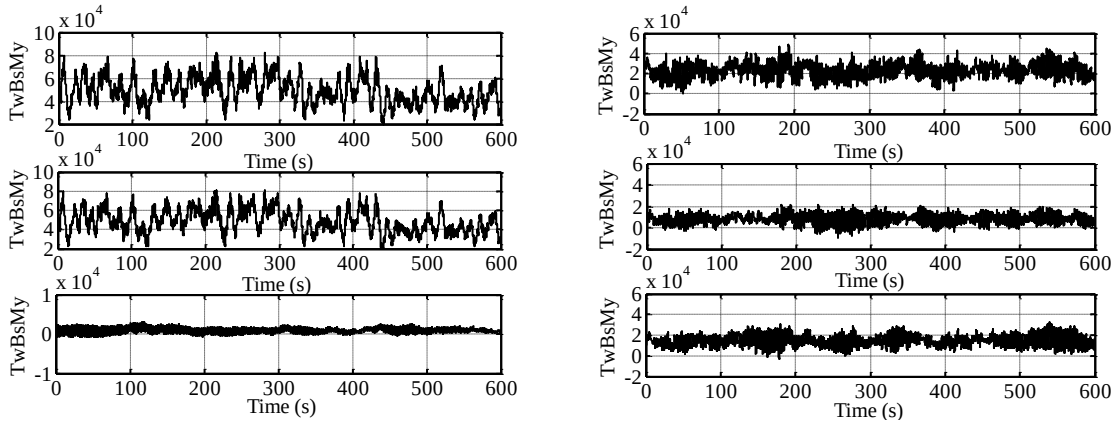

(a) Operation, U_{hub} = 13 m/s (b) Parked (standstill), U_{hub} = 50 m/s

Fig. 3 Time history samples of tower base FA bending moment from Cases 1, 2 and 3 (from top to bottom; unit of moment: kNm)

3. Analysis of dynamic wind turbine response

3.1 Roles of the wind loads on turbine blades and tower

Three different dynamic response analyses were carried out with three different considerations of wind loads: Case 1: Wind loads on both the tower and blades; Case 2: Wind loads on the blades only; and Case 3: Wind load on the tower only. The influence of gravity to the turbine response at standstill was removed from Case 3. At each wind speed, 100 wind turbulence samples were simulated by spectral representation method. The duration of wind speed sample was 630 s with time step of 0.05 s. The 100 corresponding turbine response time histories were calculated by FAST code with time step of 0.0125 s and the first 30 s of response time history was removed to eliminate startup transient. Fig. 3 shows the time history samples of tower base FA bending moment (TwBsMy) from Cases 1, 2 and 3 with mean wind speeds of 13 and 50 m/s at operational and parked conditions, respectively. It is observed that the wind load on tower only generates very small response compared to that from Cases 1 and 2 during operation, but it has significant influence on the tower response of parked turbine.

Fig. 4 shows the comparison of power spectral density (PSD) functions of blade root out-of-plane bending moment (RootMy) and tower base FA bending moment (TwBsMy) from Cases 1 and 2, which were estimated by an ensemble average of 100 samples. It is seen that, at operational condition, the blade root out-of-plane bending moment is dominated by rotor revolution frequency (1P = 0.2Hz) and its harmonics, which are due to "rotational sampled spectrum" of wind turbulence seen by the rotating blades, which is significantly different from the fixed point wind spectrum. Due to a large aerodynamic damping in flap-wise modes, the corresponding modal frequencies are not very noticeable. The tower response is dominated by the fundamental modal frequency. The 3P frequency is also observed in the tower base FA and SS bending moments. The response PSDs from Cases 1 and 2 are almost identical as shown in Fig.

4(a). At normal parked condition, both the blade and tower responses show the dominant frequencies of 1st tower FA and 1st edge-wise modal vibrations, indicating a coupling between the vibrations of tower and blades. The PSDs of the blade root out-of-plane bending moment from Cases 1 and 2 are almost identical as shown in Fig. 4(b). The PSD of the tower base FA bending moment from Case 2 is smaller than that from Case 1 at low frequency, especially at the 1st tower FA modal frequency, where the PSD from Case 1 is about three times larger than that from Case 2.

The rotor revolution frequency and its harmonics observed in the PSD of blade root out-of-plane bending moment of operational turbine are caused by both inertial force of the rotating blades and wind turbulence. To examine the influence of wind turbulence, analysis of operational turbine at vacuum (no aerodynamic force but with inertial force on the rotating blades) is also carried out.

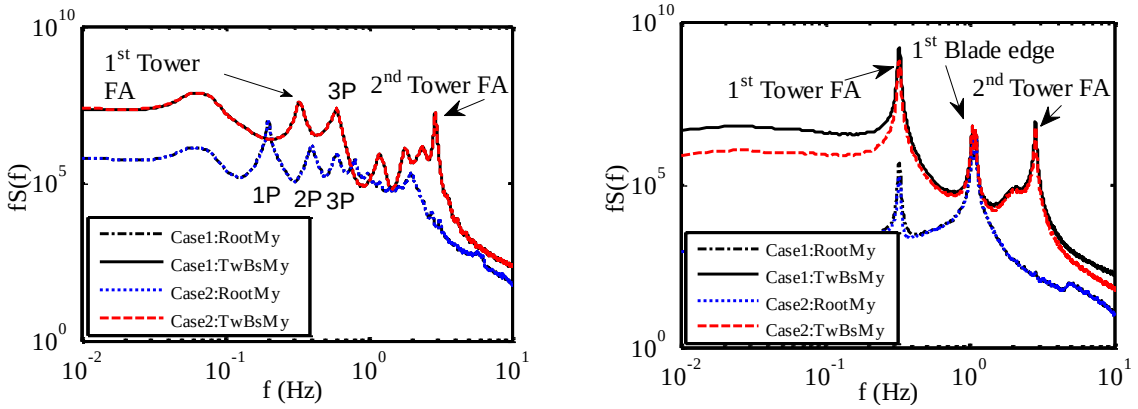

(a) Operation, U_{hub} = 13 m/s (b) Park (standstill), U_{hub} = 50 m/s

Fig. 4 PSDs of the blade out-of-plane bending moment (RootMy) and tower based FA bending moment (TwBsMy) at operational and parked conditions

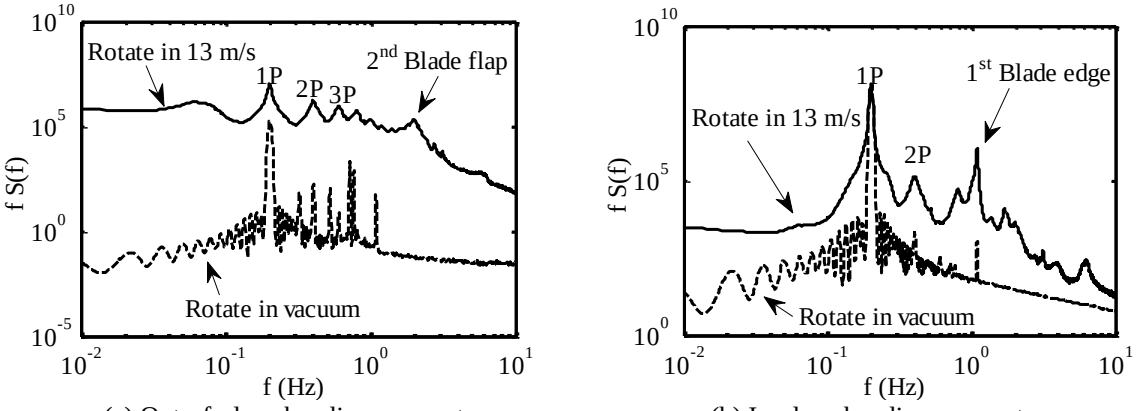

(a) Out-of-plane bending moment (b) In-plane bending moment

Fig. 5 Influence of inertial force of rotating blades and turbulence on blade root bending moments

Table 1 Ratios of the mean extreme responses from Cases 2 and 3 to Case 1 (%)

	Operational condition					Parked condition				
	U_{hub}	RootMx	RootMy	TwBsMx	TwBsMy	U_{hub}	RootMx	RootMy	TwBsMx	TwBsMy
Case 2	7 m/s	100.0	100.0	100.0	99.5	25 m/s	100.0	98.6	100.0	44.0
	13 m/s	100.0	100.0	100.0	99.0	40 m/s	100.0	96.8	100.0	49.0
	25 m/s	100.0	100.0	100.0	95.8	50 m/s	100.0	96.2	100.0	48.6
Case 3	7 m/s	0.0	0.0	0.0	2.8	25 m/s	0.0	12.9	0.0	68.7
	13 m/s	0.0	0.3	0.0	3.2	40 m/s	0.0	19.6	0.0	66.1
	25 m/s	0.0	1.1	0.0	13.4	50 m/s	0.0	23.8	0.0	66.1

This case study is different from the condition of no wind, in which the aerodynamic force on the rotating blades is not completely diminished. As shown in Fig. 5, the blade root out-of-plane bending moment and the tower FA bending moment are primarily caused by rotationally sampled turbulence, while the blade root in-plane bending moment and the tower SS bending moment are caused by the inertial force of rotating blades.

Table 1 shows the ratios of mean extreme responses (including time-invariant mean component) estimated from Cases 2 and 3 to Case 1 at operational and parked conditions through an ensemble average of 100 simulated samples. It is observed that the blade responses calculated from Case 2 are almost identical to those from Case 1, which confirmed that the wind load on the tower has a negligible effect on the blade responses at both operational and parked conditions. The difference is up to 4% as seen in the blade root out-of-plane bending moment with mean wind speed of 50 m/s at parked condition. It is also noted that the wind load on the tower has a negligible influence, as compared to the loads transferred from blades, on the tower base bending moments at operational condition. However, its influence is significant on the tower base FA response at normal parked condition. In the normal parked condition, the wind load on the tower contributes more response to total tower base FA response than that from the wind load on blades.

3.2 Characteristics of tower response

Fig. 6 shows the mean (static) and mean peak dynamic (excluding the static response) components of the tower FA bending moment and shear force at different tower elevations calculated from Cases 1, 2 and 3 at operational condition, which are estimated by an ensemble average of 100 samples. It is observed that the tower FA responses at operational condition are primarily caused by the wind loads acting on blades. Fig. 7 displays the peak and gust response factors. The peak and gust response factors of the tower base FA bending moment are 3.07 and 1.72, respectively. They are 2.98 and 1.86 for the tower base FA shear force. The peak and gust response factors are almost same over the tower elevation except at the tower top. Due to the small mean FA bending moment at the tower top, the gust factor is large at the tower top, which is 5.21. It is also noted that the mean tower response is larger than the mean peak dynamic response (excluding the mean component) along the tower elevation, except at the tower top.

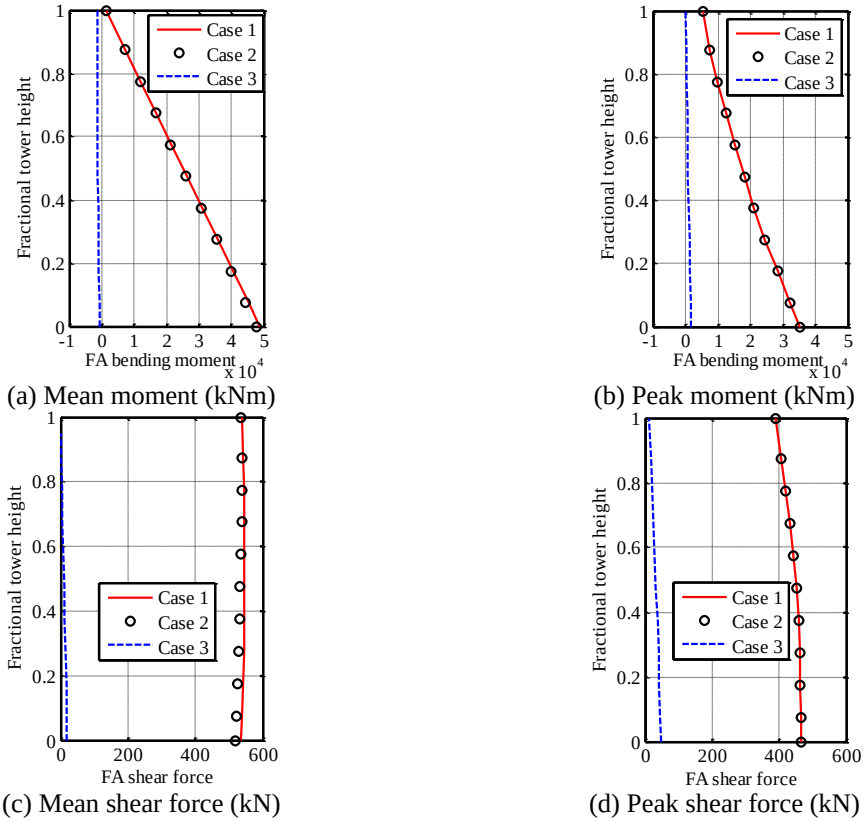

Fig. 6 Mean and peak tower FA bending moments and shear forces at operational condition (U_{hub} = 13 m/s)

The results for parked turbine are shown in Figs. 8 and 9. The wind load on the tower has a significant influence on the tower FA response. The tower FA responses calculated from Cases 2 and 3 can be combined using a combination rule for the estimation of response predicted from Case 1. The mean tower responses can be linearly added together, which is identical to that of Case 1, as shown in Figs. 8(a) and 8(c). For the tower mean peak dynamic responses, two combination rules are compared: 1) linear summation based on the assumption that dynamic responses from Cases 2 and 3 are fully correlated (DNV and Risø 2002); 2) SRSS rule based on the assumption that they are statistically independent. As shown in Figs. 8(b) and 8(d), the linear summation generally overestimates the tower FA peak dynamic bending moment as compared to that from Case 1 with differences of 25.9% and 26.5% at the tower base and top, respectively. The differences are 26.8% and 31.2% in the tower FA peak dynamic shear force at the base and top. The SRSS rule gives satisfactory predictions. The tower FA peak dynamic bending moment at the tower base and top are only overestimated by 3.5% and 0.5%. The errors are 4.0% and 1.0% for the tower FA peak dynamic shear force at the base and top. For the parked turbine, the tower base FA bending moment excited by wind load on the tower is larger than that excited by the wind load on blades. It is also noted that the mean tower response is smaller than the mean peak dynamic response along the tower elevation.

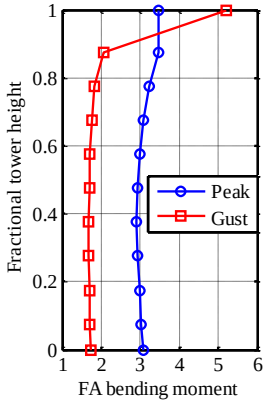

(a) Tower FA bending moment

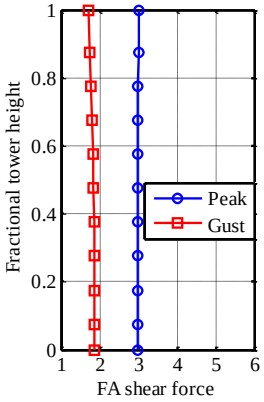

(b) Tower FA shear force

Fig. 7 Peak and gust response factors of the tower FA bending moment and shear force at operational condition (U_{hub} = 13 m/s)

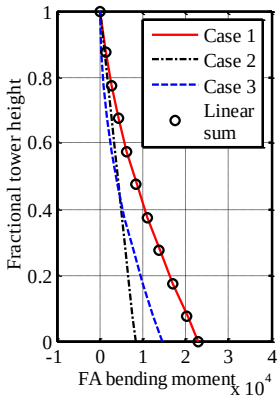

(a) Mean moment (kNm)

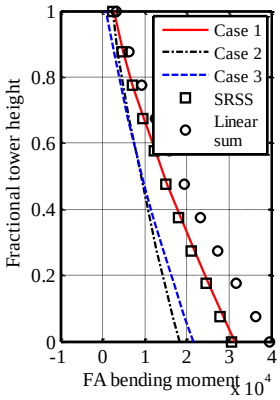

(b) Peak moment (kNm)

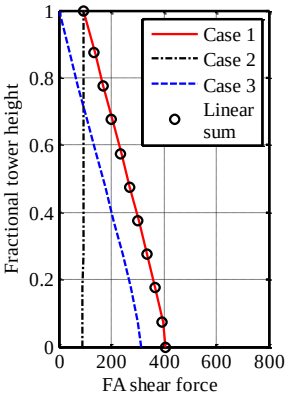

(c) Mean shear force (kN)

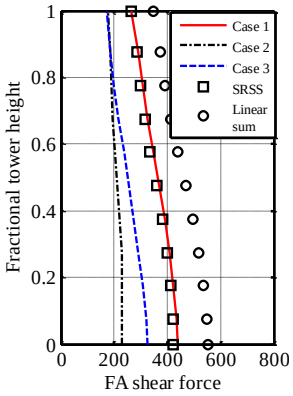

(d) Peak shear force (kN)

Fig. 8 Mean and peak tower FA bending moments and shear forces from Cases 1, 2 and 3 at parked condition (U_{hub} = 50 m/s)

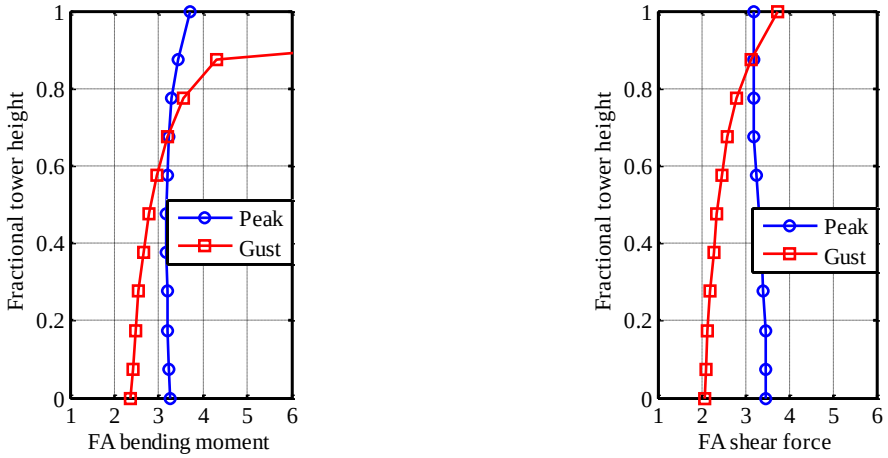

(a) Tower FA bending moment (b) Tower FA shear force

Fig. 9 Peak and gust response factors of the tower FA bending moment and shear force at parked condition (U_{hub} = 50 m/s)

As shown in Fig. 9, the gust and peak response factors are 2.37 and 3.25 for the tower base FA bending moment, respectively, and 2.07 and 3.48 for the tower base FA shear force. The peak factor over the tower elevation is almost identical, while the gust response factor increases with the tower elevation. Due to the small mean FA bending moment at the tower top, the gust response factor of 16.2 is large at the tower top.

3.3 Modeling of ESLs on tower

In current wind turbine tower design practice, the dynamic loads transferred from rotor to tower are often represented in terms of ESLs. With this modeling, the mean peak dynamic tower response due to the wind loads on blades, i.e., the response in Case 2, can be calculated using a static analysis procedure. This response is then combined with the tower extreme response under wind load on tower only, i.e., the response in Case 3, for the estimation of total tower extreme response.

From the variation of gust response factor, it is seen that the gust response factor approach for defining ESL in terms of mean load multiplied by the gust response factor is less accurate. A more adequate ESL modeling can be defined by a concentrated force and a bending moment on the tower top, and distributed fundamental modal inertial force along the tower elevation (e.g., Chen and Kareem 2004, Huang and Chen 2007). The simulation results of Case 2 show that the correlation coefficient of the tower top bending moment and shear force is quite small. It is 0.07 for the tower top FA bending moment and shear force at operational condition with mean wind speed of 13 m/s. The correlation coefficient is 0.13 for the tower top SS bending moment and shear force. For parked turbine with mean wind speed of 50 m/s, the correlation coefficient is 0.27 for the tower top FA bending moment and shear force, and 0.17 for the tower top SS bending moment and shear force.

Three ESL models were established and are compared based on the estimated mean peak

dynamic response of Case 2:

1) ESL 1: Concentrated shear force, F_{T}, and bending moment M_{T}, i.e., the mean peak dynamic responses at tower top, as shown in Fig. 10(a). The tower responses, R_{F_T} and R_{M_T}, generated from F_{T} and M_{T} are combined by the SRSS rule for the total tower response, i.e., $\sqrt{R_{F_T}^2 + R_{M_T}^2}$;

2) ESL 2: Concentrated shear force, F_{T}, and bending moment M_{T}, defined in ESL 1, with an additional distributed fundamental modal inertial force along the tower elevation, $\bar{F}_a(z) = (2\pi f_1)^2 m(z)\phi_1(z)X_{1\max}$, where f_1 is the fundamental frequency of the tower; $m(z)$ is the mass per unit height of the tower; $\phi_1(z)$ is the first tower mode shape and $\phi_1(z) = 1$ at the tower top; and $X_{1\max}$ is the mean peak dynamic displacement at the tower top, as shown in Fig. 10(b). The tower responses, R_{F_T}, R_{M_T} and $R_{\bar{F}_a}$, generated from F_{T}, M_{T} and $\bar{F}_a$ are combined using the SRSS rule for the total tower response, i.e., $\sqrt{R_{F_T}^2 + R_{M_T}^2 + R_{\bar{F}_a}^2}$. It is noted that the response $X_{1\max}$ includes the contributions of the first and second modes of tower vibration in the respective direction. As the tower response generated from $\bar{F}_a$ is secondary as compared to those from F_{T} and M_{T}, an approximate modeling of the inertial load on the tower following the fundamental (first) mode shape is considered to be adequate;

3) ESL 3: Concentrated shear force, F_{T}, is divided into a shear force, $F_T^{'}$, and an inertial force of structure components above the tower, $F_{aT} = (2\pi f_1)^2(M_b + M_N)X_{1\max}$, where M_b and M_N are the masses of blades and nacelle, by the SRSS rule, $F_T = \sqrt{F_T^{'2} + F_{aT}^2}$, and others are same as ESL 2, as shown in Fig. 10(c). The tower responses, $R_{F_T^{'}}$, R_{M_T}, $R_{F_{a\mathrm{T}}}$ and $R_{\bar{F}_a}$, generated from $F_T^{'}$, M_{T}, $F_{a\mathrm{T}}$ and $\bar{F}_a$ are combined as $\sqrt{R_{F_T^{'}}^2 + R_{M_T}^2 + \left(R_{F_{a\mathrm{T}}} + R_{\bar{F}_a}\right)^2}$. It is noted that the total tower response from ESL 3 has an additional term, $2R_{F_{a\mathrm{T}}}R_{\bar{F}_a}$, as compared with that from ESL 2.

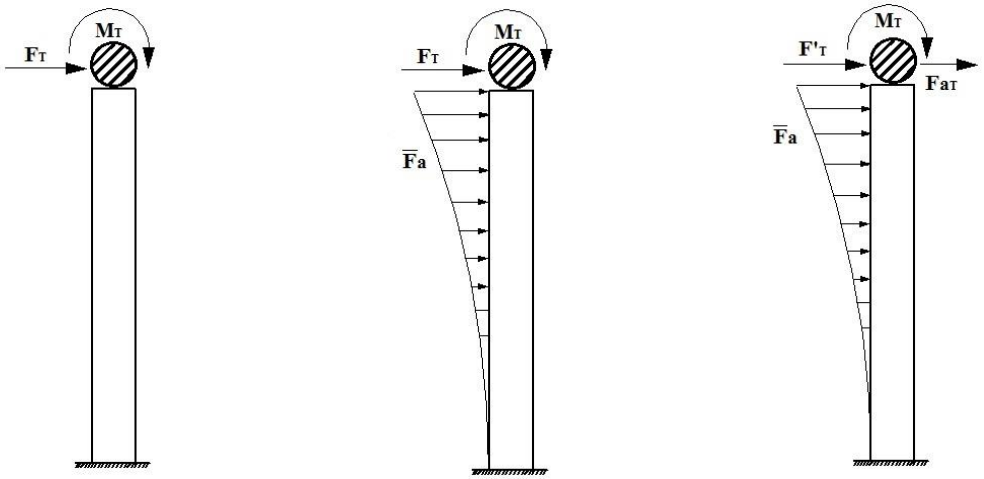

(a) ESL 1 (b) ESL 2 (c) ESL 3

Fig. 10 Models of ESLs to represent the tower dynamic responses at Case 2

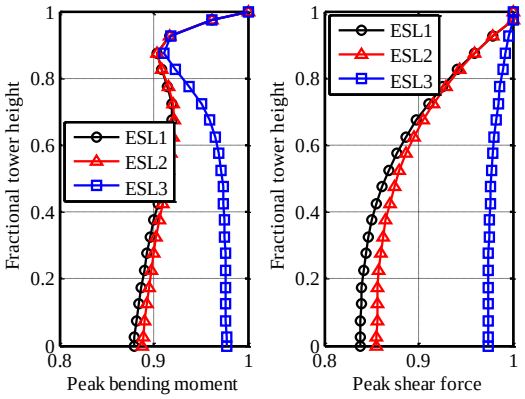

(a) FA dynamic response

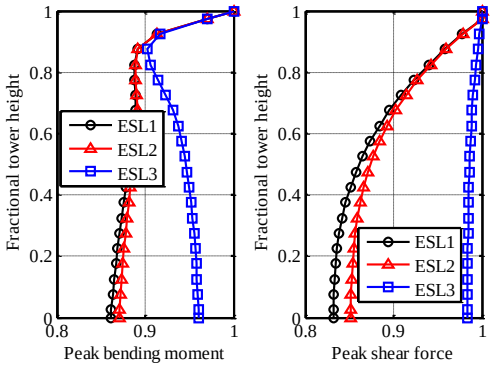

(b) SS dynamic response

Fig. 11 Comparison of the tower peak dynamic responses between ESLs and Case 2 at operational condition (U_{hub} = 13 m/s)

Table 2 shows the loads on the tower top at operational (U_{hub} =13 m/s) and parked conditions (U_{hub} =50 m/s). The peak dynamic tower responses calculated from these ESLs are compared to those from the simulations in Case 2. Figs. 9 and 10 show the ratio of the tower peak dynamic responses by ESLs to that through the simulations in Case 2. Table 3 shows the response ratios at the tower base. As expected, these three ESLs can well represent the tower top peak dynamic response. The estimations of ESLs 1 and 2 are almost same and are lower. The response caused by the fundamental modal inertial force $\bar{F}_a(z)$ is small when the SRSS rule is used to combine it with the responses from the top shear force and moment, F_{T} and M_{T}. ESL 3 leads to an improved estimation of the tower response. The difference between ESLs 2 and 3 is that the correlation between the responses caused by $\bar{F}_a(z)$ and by F_{T} is included via a linear summation of the responses from $\bar{F}_a(z)$ and F_{aT}. Therefore, the estimations of bending moment and shear force are increased as compared to ESL 2. Without the consideration of $\bar{F}_a(z)$, ESLs 2 and 3 will give same predictions. Similar results are observed in the tower SS responses as shown in Figs. 11(b) and 12(b) for operational and parked conditions, respectively. It is also noted that the largest

underestimation of the tower FA bending moment from ESL 3 is about 9%, which is observed at the higher tower level close to the tower top, where the tower bending moments generated by the tower top shear force and bending moment are quite close. Therefore, the SRSS rule of combining the responses from F_T and M_T results in a larger approximation as the tower top shear force and bending moment are not completely independent.

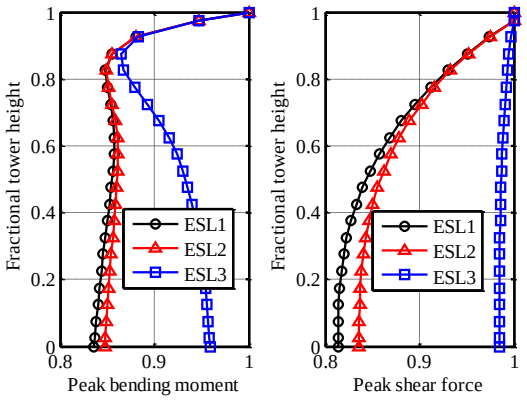

(a) FA dynamic response

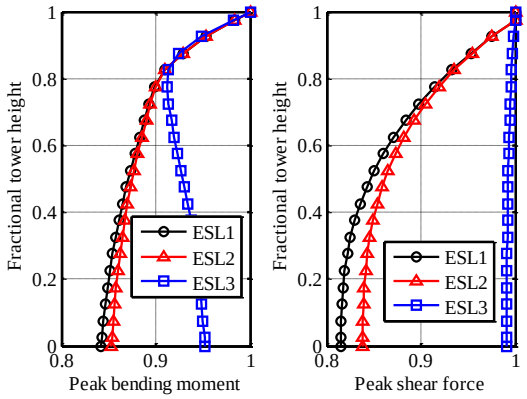

(b) SS dynamic response

Fig. 12 Comparison of the tower peak dynamic responses between ESLs and Case 2 at parked condition (U_{hub} = 50 m/s)

Table 2 ESL from the simulated peak dynamic responses of Case 2

Condition	Direction	F_T (kN)	M_T (kNm)	Fa_T (kN)	F'_T (kN)
Operation	FA	389.3	5471.5	292.5	256.9
(13 m/s)	SS	86.6	888.6	65.8	56.3
Park	FA	178.4	2425.4	154.7	88.9
(50 m/s)	SS	342.5	6101.1	290.9	180.7

Table 3 Ratios of the tower base peak dynamic responses from ESLs 1, 2 and 3 to that from Case 2

	ESLs	Operational condition (U_{hub} = 13 m/s)				Parked condition (U_{hub} = 50 m/s)			
		FA moment	FA force	SS moment	SS force	FA moment	FA force	SS moment	SS force
Tower base	ESL 1	0.88	0.84	0.86	0.83	0.84	0.81	0.84	0.82
	ESL 2	0.89	0.86	0.87	0.85	0.85	0.84	0.85	0.84
	ESL 3	0.98	0.97	0.96	0.98	0.96	0.98	0.95	0.99

4. Conclusions

The dynamic response analysis of both operational and parked wind turbines was conducted using the onshore 5-MW baseline wind turbine in order to gain better understanding of the response characteristics of turbine system. The wind load on the tower has a negligible effect on both the tower and blade responses under operational condition and on the blade response at parked condition. However, it has a significant influence on the tower fore-aft response at parked condition. The PSDs of the blade responses are dominated by the rotor revolution frequency during operation, which is associated with rotationally sampled wind turbulence. The PSDs of the tower responses are dominated by the tower fundamental frequencies with coupled rotor edgewise modal frequencies. For a parked turbine, the tower fore-aft response due to the wind loads on blades and tower can be estimated separately and then combined by using the SRSS rule for the estimation of total response. The current linear summation rule used in some design codes was proved to be over-conservative.

Three ESL models were compared with different considerations of the concentrated force and moment at the tower top, and the distributed fundamental inertial force along the tower elevation. These ESL models were used to estimate the tower response due to wind loads on blades only. The new ESL model introduced in this study, i.e., ESL3, has resulted in an improved prediction of the tower response. The ESL model facilitates load (response) combinations which are essential for tower design.

Acknowledgements

The support for this work, provided in part, by NSF Grant No. CMMI-1029922 is greatly acknowledged.

References

Blaise, N. and Denoel, V. (2013), "Principal static wind loads", *J. Wind Eng., Ind. Aerod.*, **113**, 29-39.

Chen, X. and Kareem, A. (2004), "Equivalent static wind loads on tall building: new model", *J. Struct. Eng. - ASCE*, **130**(10), 1425-1435.

Chen, X. and Kareem, A. (2005), "Proper orthogonal decomposition-based modeling, analysis and simulation of wind loads and their effects", *J. Eng. Mech. -ASCE*, **131**(4), 325-339.
DNV and Risø. (2002), *Guidelines for design of wind turbines*, 2nd Ed., Denmark.
Huang, G. and Chen, X. (2007), "Wind load effects and equivalent static wind loads of tall building based on synchronous pressure measurements", *Eng. Struct.*, **29**, 2641-2653.
Holmes, J.D. (2002), "Effective static load distributions in wind engineering", *J. Wind. Eng. Ind. Aerod.*, **90**, 91-109.
International Electrotechnical Commission (2005), *Wind Turbines-Part 1: Design Requirement*, IEC 61400-1 Edition 3, HIS, Geneva, Switzerland.
Jonkman, J.M. and Buhl Jr, M.L. (2005), "FAST User's Guide", National Renewable Energy Laboratory, Golden, Colorado, USA, Report NREL/EL-500-38230.
Jonkman, J.M., Butterfield, S., Musial, W. and Scott, G. (2009), "Definition of a 5-MW Reference Wind Turbine for Offshore System Development", National Renewable Energy Laboratory, Golden, Colorado, USA, Report NREL/TP-500-38060.
Katsumura, A., Tamura, Y. and Nakamura, O. (2007), "Universal wind load distribution simultaneously reproducing largest load effects in all subject members on large-span cantilevered roof", *J. Wind Eng. Ind. Aerod.*, **95**, 1145-1165.
Li, Y.Q., Wang, L., Tamura, Y. and Shen, Z.Y. (2009), "Universal equivalent static wind load estimation for spatial structures based on wind-induced envelope responses", *Symposium of the International Association for Shell and Spatial Structures*, Valencia, Spain, September 28 - October 2.
Moriarty, P.J. (2008), "Database for validation of design load extrapolation techniques", *Wind Energy*, **11**(6), 559-576.
Moriarty, P.J. and Hansen A.C. (2005), "AeroDyn theory manual", NREL/TP-500-36881, Golden, Colorado.
Murtagh, P.J., Basu, B. and Broderick, B.M. (2005), "Along-wind response of a wind turbine tower with blade coupling subjected to rotationally sampled wind loading", *Eng. Struct.*, **27**, 1209-1219.
Shinozuka, M. and Deodatis, G. (1996), "Simulation of multidimensional Gaussian stochastic fields by spectral representation", *Appl. Mech. Rev.*, **49**(1), 29-53
Zhou, X., Gu, M. and Li, G. (2011), "Application research of constrained least-squares method in computing equivalent static wind loads", *Proceedings of the 13th International Conference on Wind Engineering*, Amsterdam, Netherlands, July 10-15.

JH